

action energy which is based on the Friedel-Anderson model.¹⁸

Our plots of $T^2\Delta C$ versus T^3 yield values of the electronic heat capacity γ which seem to be much too large compared to any reasonable numbers that can be derived from the Friedel-Anderson model. In fact, it seems to be quite a common occurrence to find unusually high increases in γ associated with magnetic impurities. There are large uncertainties in trying to separate the magnetic contribution from measured heat-capacity data in order to arrive at that contribution which is linear in temperature (presumably electronic). Probably for this reason we have been unable to find systematic experimental measurements of changes in γ associated with magnetic impurities. Yet examination of published data of others as well as some of our own taken on Fe in Mo would indicate that unreasonably

¹⁸ B. Caroli, *J. Phys. Chem. Solids* **28**, 1427 (1967).

large increases in γ occur.¹⁹ For example, Fig. 3 of the paper of du Chatenier and de Nobel¹⁵ suggests an increase $\Delta\gamma/\gamma_{Ag}$ of ~ 1 for ~ 0.001 parts of Mn in Ag. Increases we estimate from the present work are almost as great; however, before serious analysis of the effect is attempted, it would be worthwhile to develop means for making measurements in more dilute alloys where corrections for magnetic ordering will be less serious.

ACKNOWLEDGMENTS

We would like to thank H. J. Williams and R. C. Sherwood for making the measurements of susceptibility and Mrs. A. S. Cooper for determining the lattice constants and for her help with preparing Table II.

¹⁹ We would like to thank P. A. Wolff for enlightening us a number of years ago as to the unreasonably large increases in density of states per Fe added to Mo that would be found if the data were processed in the obvious way.

Sublattice Magnetization in FeF₃ near the Critical Point

G. K. WERTHEIM, H. J. GUGGENHEIM, AND D. N. E. BUCHANAN

Bell Telephone Laboratories, Murray Hill, New Jersey

(Received 28 December 1967)

The ⁵⁷Fe Mössbauer effect has been used to measure the sublattice magnetization $M(T) = M_0 D(1 - T/T_N)^\beta$ of FeF₃ in the region $0.85 < T/T_N < 0.9995$. The behavior in the critical region yields $\beta = 0.352 \pm 0.005$ and $D = 1.207 \pm 0.015$. The critical exponent differs appreciably from those reported in MnF₂ and FeF₂ but is similar to those reported for liquid-vapor transitions and for other ferromagnets.

THERE is currently a great deal of interest in the behavior of physical systems near their critical points.¹ Striking similarities exist between the liquid-vapor transition in both classical and quantum liquids and the magnetic transition in solids. Measurements in liquids extend much closer to the critical point than those in magnetic solids, but in neither case is the precision sufficient to show whether there is indeed a common value for the critical point coefficients.

In this work we are concerned with the sublattice magnetization of an antiferromagnet in the region just below the Néel point. In the critical region the temperature dependence of the magnetization is described by the equation

$$M(T) = M_0 D(1 - T/T_N)^\beta, \quad (1)$$

where β is the critical exponent, M_0 the saturation value of the magnetization, and D a factor near unity which represents the misfit between this expression and the behavior of real substances at zero degrees. It is sensitive to such factors as the details of the spin-wave

spectrum, e.g., the spin-wave gap at $k=0$ and the spin-wave dispersion. These do not appear to affect the critical exponent,² in agreement with a conjecture used in the derivation of certain scaling laws.¹

In the present experiment we use the Mössbauer effect of ⁵⁷Fe to measure the sublattice magnetization of FeF₃, a canted antiferromagnet.³ According to x-ray crystallographic work,⁴ FeF₃ belongs to the space group $R\bar{3}c$ and has a bimolecular rhombohedral unit cell. The structure may be visualized as regularly spaced parallel planes perpendicular to the $[111]$ direction, alternately occupied by iron atoms and fluorine atoms. All metal atoms are crystallographically equivalent and lie on threefold axes. The local environment of the iron atoms consists of six fluorine neighbors which form an almost regular octahedron. They have six equidistant iron neighbors. The antiferromagnetic character was established by neutron diffraction,⁵ which also

² G. K. Wertheim and D. N. E. Buchanan, *Phys. Rev.* **161**, 478 (1967).

³ T. Moriya, *Phys. Rev.* **120**, 91 (1960).

⁴ M. A. Hepworth, K. H. Jack, R. D. Peacock, and G. J. Westland, *Acta Cryst.* **10**, 63 (1957).

⁵ E. O. Wollan, H. R. Child, W. C. Koehler, and M. K. Wilkinson, *Phys. Rev.* **112**, 1132 (1958).

¹ See L. P. Kadanoff *et al.* [*Rev. Mod. Phys.* **39**, 395 (1967)] for a comparison of theory and experiment very near critical points.

suggested that the spins are parallel to the (111) planes.

Mössbauer experiments on FeF_3 were first reported by us some years ago⁶ but a detailed analysis of the temperature dependence of the sublattice magnetization was not made because of the coexistence of paramagnetic and antiferromagnetic material over a significant range of temperature. The same problem has recently been encountered in other Mössbauer experiments dealing with the critical point behavior of FeF_3 ⁷ and FeOOH .⁸ In the present work⁹ this problem has been entirely overcome by the use of better material.

The sublattice magnetization of FeF_3 is measured in terms of the hyperfine interaction of the trivalent iron ions, which have the $3d^5$, $^6S_{5/2}$ configuration. In such an ion, the effective field at the nucleus arises almost entirely from core polarization by the half-filled $3d$ shell. The quadrupole splitting was found to be small (Appendix A), which indicates that dipolar fields are also small. The hfs magnetic field, H , is therefore a good measure of the z component of the d -electron spin and of the sublattice magnetization provided the hfs coupling constant is independent of the magnetization. Under these circumstances one can replace M by H in Eq. (1). The linewidths of the Mössbauer spectra indicate that the spin relaxation time is sufficiently short so that a true time-average field exists at the nucleus, i.e., the spin relaxation time is much shorter than the Larmor period.

EXPERIMENTAL

The FeF_3 was in the form of a green microcrystalline powder. It was prepared from high purity $\text{Fe}(\text{NO}_3)_3 \cdot 9\text{H}_2\text{O}$, which was first converted to a hydrated fluoride, and then to the anhydrous salt by heating in HF at 900°C. The Mössbauer spectra showed only the expected six magnetic hfs lines. Impurities were not detectable. The linewidths obtained were 0.026–0.030 cm/sec before correction for finite absorption broadening, except in the immediate vicinity of the Néel point where other mechanisms contribute to the linewidth (see below).

The absorber was made of small crystals of FeF_3 imbedded in an epoxy binder. Data taken with bare powder did not differ in any way from those obtained with the cast plastic absorber. The sample had a copper-constantan thermocouple imbedded in it about one third of the distance from the edge to the center. It was wrapped in two layers of 5×10^{-4} cm aluminum foil and mounted in the center of a tubular stainless-steel furnace insert 6 cm long, inside which the control

thermocouple was attached. The furnace insert was closed off with two additional layers of aluminum foil at each end. This assembly was placed in a furnace which was then also closed with aluminum foils. The control thermocouple was used to switch the furnace power between two levels. The temperature swing at the control thermocouple was 0.05°C and that of the sample thermocouple appreciably smaller, i.e., $\delta T/T_N \sim 10^{-4}$.

It is important to consider to what extent temperature fluctuations and temperature inhomogeneities in the absorber affect the data. Differentiating the equation for the temperature dependence of the sublattice magnetization yields

$$\delta H/H = \delta M/M = -\beta \delta T / (T_N - T). \quad (2)$$

With $\delta T/T_N \sim 10^{-4}$ and $1 - T/T_N = 10^{-3}$ one obtains a spread in H of 3%, or 3 kOe, which results in only slight line broadening. Additional broadening could arise from a spread in temperature across the absorber, or from a distribution of Néel temperatures in the crystallites due to chemical or crystallographic imperfections. The latter will produce line broadening near the Néel temperature indistinguishable from that due to a temperature distribution. The results in Ref. 7 suggest that this may be a serious problem. We cannot rule out a residual spread of 0.06 °K in the Néel temperature in this experiment.

The Mössbauer spectrometer was of the conventional constant acceleration type,¹⁰ operating with a symmetrical sawtooth waveform having a period of 0.16502 ± 0.00001 sec. This waveform is made by an integrator without low-frequency cutoff operating between limits defined by carefully matched and temperature-compensated Zener diodes.¹¹ The multi-channel analyzer is operated as a crystal clock controlled multiscaler with 400 μ sec dwell time and 12.5 μ sec dead time, corresponding to a period of 0.1646 sec for 399 channels. The frequency of the waveform generator was chosen so as to make the velocities represented by channels $200 - n$ equal to that of channels $201 + n$; $n = 0, 1, \dots, 199$. This allows one to add the spectra obtained in the two halves of the analyzer without line broadening. The electromechanical transducer employed a 15 cm LVsyn¹² as a velocity sensor because of its superior linearity. Loudspeakers are generally nonlinear because the magnetic field acting on the voice coil is a function of voice-coil displacement. This may be a significant source of nonlinearity and results in incompatibility between the two spectra because the average position of the voice coil is different in the two halves of the motion. Zero position drift has been eliminated by replacing the dc-coupled power amplifier by a current booster within the feedback loop. The

⁶ D. N. E. Buchanan and G. K. Wertheim, *Bull. Am. Phys. Soc.* **7**, 227 (1962); and in *Mössbauer Effect, Principles and Applications* (Academic Press Inc., New York, 1964), pp. 73 and 100.

⁷ U. Bertelsen, J. M. Knudsen, and H. Krogh, *Phys. Status Solidi* **22**, 59 (1967).

⁸ F. van der Woude and A. J. Decker, *Phys. Status Solidi* **9**, 775 (1965); **13**, 181 (1966).

⁹ A preliminary account of this work has been published in *Solid State Commun.* **5**, 537 (1967).

¹⁰ G. K. Wertheim, *Mössbauer Effect, Principles and Applications* (Academic Press Inc., New York, 1964), Chap. 2.

¹¹ R. L. Cohen, *Rev. Sci. Instr.* **37**, 260 (1966); **37**, 977 (1966).

¹² Trademark of Sanborn Division of Hewlett-Packard.

calibration constant of this instrument has remained stable to within 1 part in 10^3 for over a year and is significantly better on a short term.

Prior to data analysis, the independent spectra obtained in the two analyzer halves were combined to eliminate the r^{-2} geometric distortion. Least-squares fits were then made using six Lorentzian lines, specified by position, width, and amplitude. See Figs. 1 and 2 for examples of the data and the fit obtained. All eighteen parameters were treated as independent variables and no constraints were imposed. This approach was found advantageous because the spin direction is not known and the quadrupole splitting is less than one tenth of the experimental linewidth. The resulting parameters were used in the following manner. The linewidths and intensities were examined as a check on the validity of the data. Some examples of these are shown in Table I. The line intensities have been normalized to add up to 6. We find little change in these relative intensities

TABLE I. Linewidths and normalized areas obtained by least-squares fitting: (a) inner lines (b) outer lines. For comparison, the table also gives results obtained with a metallic iron absorber.

Temperature (°K)	Linewidth (cm/sec)		Area ratios
	(a)	(b)	
4.2	0.0259	0.0276	1.15:2.07:2.78
308.16	0.0254	0.0269	1.15:1.94:2.91
341.43	0.0277	0.0285	1.17:1.94:2.90
357.43	0.0282	0.0306	1.19:1.94:2.88
361.47	0.0293	0.0342	1.18:1.92:2.90
362.70	0.0336	0.0419	1.28:2.06:2.66
363.44		0.0364	
	0.0025 cm Fe absorber		
296°K	0.0246	0.0288	1.19:2.05:2.76

between 4.2°K and 361.5°K, i.e., to within 1.6°K of the Néel point.

Within 0.4°K of the Néel point the intensity of the outer lines has decreased by 8% and the linewidth has increased by 50%. The loss of intensity by the outer lines is a reflection of the asymmetrical line shape produced by the highly nonlinear change of magnetization with temperature near the critical point. The results indicate a combined spatial, temporal, and Néel temperature spread of $\sim 0.1^\circ\text{K}$. Within 0.17°K of the Néel point the two inner lines were no longer resolved and the hyperfine field obtained must be considered to be an upper limit of the true field. We must emphasize, however, that we do not find any region of temperature in which magnetically ordered and paramagnetic material coexist. This is in pronounced contrast to the results of Ref. 7. In the light of our earlier experience⁶ such results are attributable to a spreading out of the Néel temperature in nonstoichiometric or impure (perhaps hydrolized) material. It would be of interest to determine whether similar results in other materials which have been attributed to a spin relaxation time

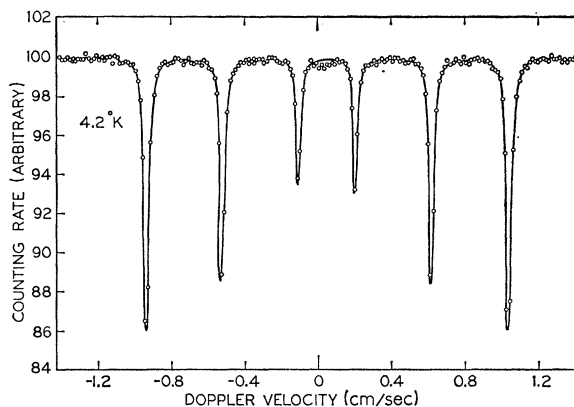


FIG. 1. Mössbauer absorption spectrum of FeF_3 at 4.2°K.

comparable to the Larmor period are in fact due to lack of crystal perfection.

The hyperfine effective field acting on the ^{57}Fe nucleus was obtained from the splitting of the ground state, which is directly available as the separation of two pairs of Mössbauer lines. Unlike the separation of the outer lines, 1_1^* and 6_1^* , the separations of 2 and 4 and 3 and 5 are independent of quadrupolar admixture and therefore provide a better measure of the hyperfine field. The results are summarized in Table II and Fig. 3.

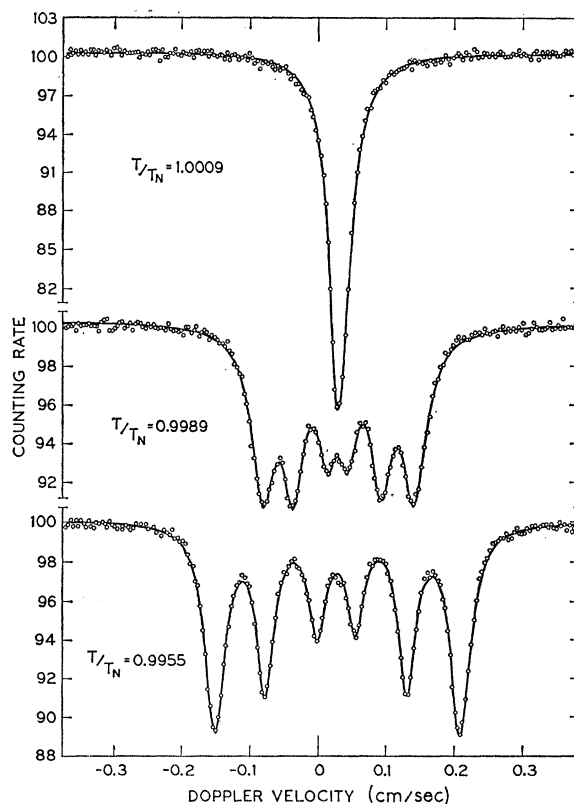


FIG. 2. Least-squares fit to Mössbauer absorption spectra of FeF_3 in the immediate vicinity of the Néel temperature.

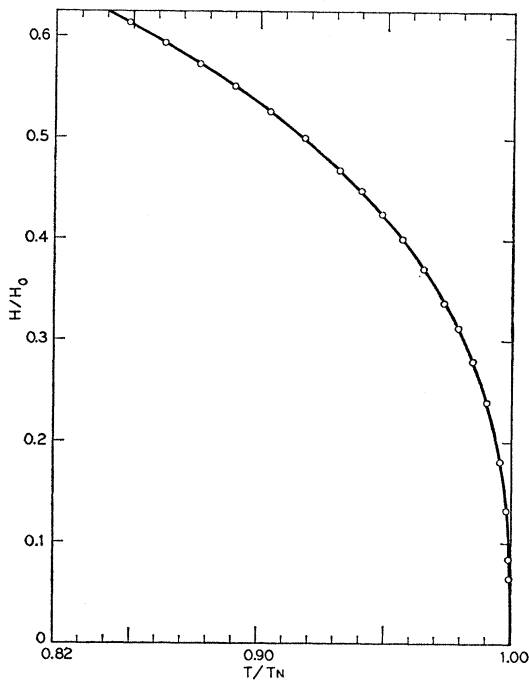


FIG. 3. Normalized sublattice magnetization of FeF_3 near the Néel point.

DISCUSSION

The ultimate objective is to compare the data with Eq. (1) in order to determine the critical exponent β , T_N , and D . The difficulties inherent in this process are well recognized.¹ They arise largely from the fact that the region of validity of this expression is not known. Moreover, if the data do not extend over a sufficient range of temperature it is possible to find a range of pairs of values of T_N and β which produce satisfactory fits.¹

The simplest approach, and one we have used previously,⁹ consists of making a plot of $\log H$ versus

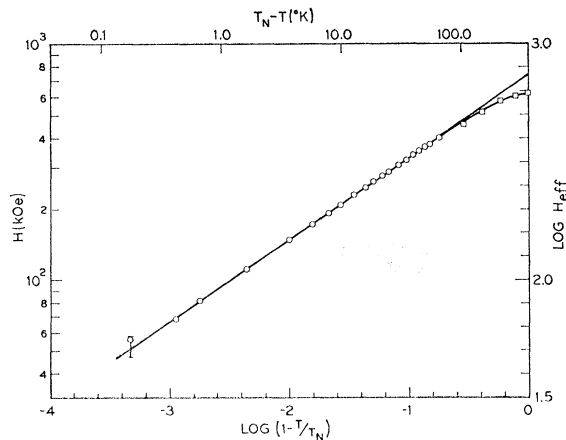


FIG. 4. Logarithmic plot of the hfs effective field against $1 - T/T_N$. The data more than 100°K from the Néel point were taken from earlier work (Ref. 6). (Base of logarithms is 10.)

$\log(1 - T/T_N)$ for a range of values of T_N and examining the quality of the fit which is obtainable with a straight line. The present data are plotted in this fashion in Fig. 4. One notes that an apparently excellent fit to the data up to $T/T_N = 0.8$ is obtained, but it is also obvious that this presentation is not even sufficiently sensitive to show the scatter inherent in the experimental points.

A much more sensitive approach is based on a transformation of Eq. (1) due to Heller,¹³ which takes the form

$$\Delta T/T_N = 1 - (T/T_N) - (H/H_0 D)^{1/\beta}, \quad (3)$$

where ΔT is the difference in temperature between an

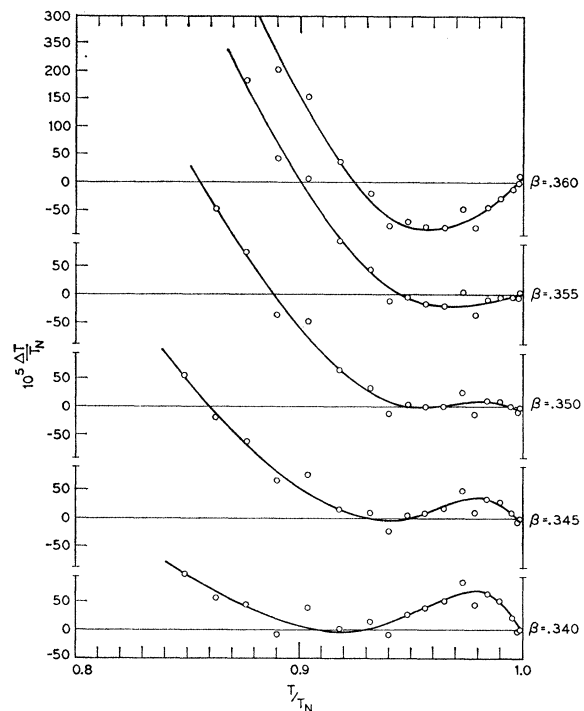


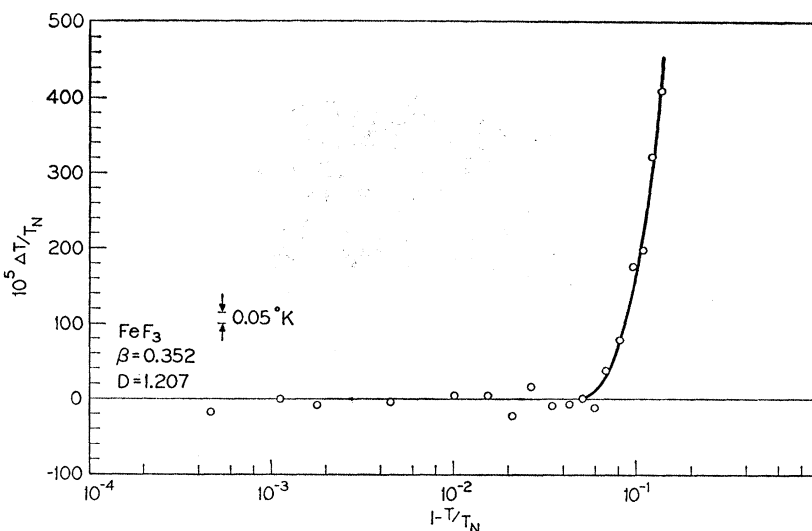
FIG. 5. The misfit between theory and experiment for various assumed values of β .

experimental point and the temperature computed from Eq. (1) for the measured field. Both the experimental error and the misfit between theory and experiment appear in ΔT . The most valuable property of a plot of $\Delta T/T_N$ versus T/T_N is that errors in the unknown parameters T_N , β , and D each produce a characteristic behavior in the resulting plot. Only an erroneous value of β will produce curvature in the critical region. An erroneous value of D merely introduces a slope, but does not affect the intercept at $T/T_N = 1.0$; the latter depends only on the choice of T_N . A second advantage is that the sensitivity can be increased arbitrarily.

In Fig. 5 we show the present data plotted in this

¹³ P. Heller, Phys. Rev. **146**, 403 (1966); P. Heller and G. B. Benedek, Phys. Rev. Letters **8**, 428 (1962).

FIG. 6. The misfit between theory and experiment for the optimum value of the critical point parameters: $\beta=0.352\pm 0.005$, $D=1.207\pm 0.015$, $T_N=363.11^\circ\text{K}$.



form on a scale chosen to be closely similar to that used by Heller, see Fig. 13 of Ref. 13. For each plot, D was adjusted to make the data intercept the T/T_N axis near 0.93. The behavior of the data as a function of β is very similar to that found in MnF_2 ,¹³ but β is here larger by ~ 0.015 .

The correct critical exponent is the one that makes ΔT vanish over the greatest possible region near the critical point. Examination of the data shown suggests that it is 0.352 ± 0.005 . The limits of error were obtained by finding the value of β at which the systematic

TABLE II. Summary of data. The probable error in the temperature is $\pm 0.05^\circ\text{K}$. The magnetic field is computed using as a calibration a ground-state splitting of 0.392 cm/sec for metallic iron at 296°K where the effective field is 330.5 kOe. Probable errors in the magnetic field are ± 0.2 kOe except in the immediate vicinity of the Néel point where they are larger.

Temperature ($^\circ\text{K}$)	Magnetic field (kOe)
362.94	<56.30
362.70	68.31
362.46	81.68
361.47	111.63
359.44	147.79
357.43	172.48
355.40	192.96
353.38	208.17
350.38	229.54
347.32	247.56
344.43	262.49
341.43	276.82
338.36	289.25
333.32	308.32
328.28	324.74
323.28	340.48
318.25	354.02
313.28	366.85
308.16	378.95
296.5	404.41
...	...
4.2	618.1

distortion of the data is comparable to the scatter in the experimental points. The value obtained for D is 1.207 ± 0.015 and that for T_N is $363.11\pm 0.05^\circ\text{K}$ relative to the other temperatures quoted in Table II. The absolute error in the temperature scale is $\pm 0.5^\circ\text{K}$. The misfit at $T/T_N=0.9$ is then 0.5°K , which is too small to see in a logarithmic plot like that of Fig. 4.

One significant criticism that can be levied against this method of data analysis is that it does not give enough weight to the data closest to the critical point. One would like to have a logarithmic temperature scale to make full use of the data in the interval $0.99 < T/T_N < 1.0$. To this end we plot $\Delta T/T_N$ versus $\log(1-T/T_N)$, with the β set equal to the optimum value determined above. The result, Fig. 6, shows a fit between theory and experiment to within $\pm 0.08^\circ\text{K}$ in the region $0.95 < T/T_N < 0.9995$. Note that the range of validity is very similar to that reported for MnF_2 . Both results suggest that determination of the critical exponent based on a fit to data in the region $0.5 < T/T_N < 0.99$ should be suspect.

The data have also been analyzed using a nonlinear least-squares program in which β , T_N , and D are treated as independent variables. The region of validity of the theoretical expression was established by finding the temperature interval below the Néel point in which the rms deviation of the measured hyperfine-field values is a minimum. By this criterion, Eq. (1) is valid within our experimental error in the interval $0.94 < T/T_N < 0.9995$. The values of the critical parameters found by this method agree well with those quoted above. They are: $\beta=0.352\pm 0.006$, $T_N=363.12\pm 0.02^\circ\text{K}$, and $D=1.208\pm 0.013$, where the quoted errors correspond to two standard deviations.

The question arises at this point whether the value of β found here differs significantly from that measured in MnF_2 , which is probably more accurately known than any other. We find that the quoted errors lead to the conclusion that the two exponents differ by a small

but significant amount. A comparison of Fig. 5 with Fig. 13 of Ref. 13 tends to reinforce that conclusion. Analysis of the MnF_2 data restricted to a region closer to the critical point¹⁴ has given a somewhat larger exponent, 0.336, but a significant difference remains. There is also an appreciable difference between the value of the critical exponent in FeF_2 ,² 0.325 ± 0.005 , and that found here, but it is not known to what extent the thermal-expansion correction will reduce this discrepancy.

On the other hand the value of β in FeF_3 does not differ significantly from those found in liquid-vapor transitions, e.g., Xe: 0.350 ± 0.015 ¹⁵ and CO_2 : 0.344 ± 0.010 ,¹⁶ or from those reported for other magnetic transitions in ferro- and antiferromagnets, e.g., YFeO_3 : 0.354 ± 0.005 ¹⁷ and CrBr_3 : 0.365 ± 0.015 .¹⁸ It is difficult to avoid the conclusion that β in FeF_3 differs significantly from the values found in the rutile structure fluorides, MnF_2 and FeF_2 . On the other hand it agrees, within the experimental error, with those reported for many other second-order phase transitions. If any experiments have demonstrated a lattice dependence in β , it is those on the rutile structure fluorides.

If β is indeed a universal constant, the body of results now available suggests that it is a number greater than $\frac{1}{3}$.¹⁹ Agreement with the 3-dimensional Ising model which yields 0.3125 is poor. We find no tendency of β to change toward the mean field theory value for $1 - T/T_c < 10^{-2}$, a phenomenon which has been reported in certain ferromagnets.

¹⁴ P. Heller, Repts. Progr. Phys. **30**, 731 (1968).

¹⁵ H. W. Habgood and W. G. Schneider, Can. J. Chem. **32**, 98 (1954).

¹⁶ H. L. Lorentzen, Acta Chem. Scand. **7**, 1335 (1953).

¹⁷ M. Eibschütz, S. Shtrikman, and D. Treves, Phys. Rev. **156**, 562 (1967).

¹⁸ S. D. Senturia and G. B. Benedek, Phys. Rev. Letters **17**, 475 (1966).

¹⁹ E. Callen and H. Callen [J. Appl. Phys. **36**, 1140 (1965)] have reported calculations for the Heisenberg model in a random-phase Green's function theory and in a two-spin cluster approximation. Both show a wide region in which M^2 is a linear function of temperature, but neither extends into the critical region. The present data, plotted as H^3 versus T , do indeed exhibit a linear region in the interval $0.8 < T/T_N < 0.97$, but show large deviations closer to the critical point. However, this analysis cannot be considered a determination of the critical exponent.

ACKNOWLEDGMENT

The authors are indebted to E. Helfand for enlightening discussions.

APPENDIX A

The isomer shift relative to a ^{57}Co in Pd source was 304 ± 6 μ/sec at 296.5°K and 265 ± 5 μ/sec just above the Néel point. (To convert to the sodium nitroprusside standard add 441 ± 5 μ/sec .) In the range of temperature from 296 to 400°K the isomer shift exhibited a temperature dependence of 0.60 μ/sec per °K, equivalent to $(1/\nu)(\partial\nu/\partial T)_p = -2.0 \times 10^{-15}$ (°K)⁻¹. This is less than the classical value of -2.46×10^{-15} (°K)⁻¹, which should be reached at higher temperature. The isomer shift is continuous at the Néel temperature to a precision of ± 2 μ/sec . A discontinuity has been reported at the Curie point of iron²⁰ where it has been attributed to a first-order component in the magnetic phase change. A number of other mechanisms for such isomer shift discontinuities have been proposed,^{21,22} but these effects are apparently not measurable in FeF_3 .

All data show a small, temperature-independent quadrupole interaction. At 4.2°K, $e^2qQ\frac{1}{2}(3\cos^2\theta - 1)$ is $+46 \pm 10$ μ/sec ; the average value obtained in the critical region is $+44 \pm 5$ μ/sec . The angle θ between the spin direction and the threefold axis is not known with certainty, but neutron scattering results suggest that the spins lie in the (111) plane, making $\frac{1}{2}(3\cos^2\theta - 1) = -\frac{1}{2}$, so that $e^2qQ = -0.0088 \pm 0.0016$ cm/sec. The quadrupole splitting in the paramagnetic state is too small compared to the natural linewidth to be resolved; it does, however, contribute to the observed linewidth.

The quadrupole splitting is small in part because the local fluorine environment is nearly octahedral. A lattice sum²³ gave an electric field gradient very much smaller than that in Fe_2O_3 , which is in agreement with the present results.

²⁰ R. S. Preston, Phys. Rev. Letters **19**, 75 (1967); R. S. Preston, S. S. Hanna, and J. Heberle, Phys. Rev. **128**, 2207 (1962).

²¹ S. Alexander and D. Treves, Phys. Letters **20**, 134 (1966).

²² J. Dlouhá, Czech. J. Phys. **B14**, 580 (1964).

²³ G. Burns (private communication).

Erratum

Paramagnetic Relaxation of Some Rare-Earth Ions in Diamagnetic Crystals, CHAO-YUAN HUANG [Phys. Rev. **139**, A241 (1965)].

1. Equations (24) and (26) should be multiplied by a factor $(2\pi^2)^{-1}$. Equation (25) should be multiplied by a factor $(4\pi^4)^{-1}$. Equation (27) should be multiplied by a factor $(32\pi^4)^{-1}$. Thanks are due to Dr. T. J. Menne and Professor A. W. Nolle for pointing out these errors.

2. Equations (24), (25), and (26) were also obtained by Dr. M. Inoue in her thesis.

3. In Fig. 5, the labels Γ_7 and $\Gamma_8^{(4)}$ should be interchanged. The author is grateful to Dr. E. S. Sabisky for pointing out the error.